Journal of Holography Applications in Physics
Volume 4, Issue 1, Winter 2024, 1-26
©Available online at http://jhap.du.ac.ir
DOI: 10.22128/JHAP.2023.757.1067
Online ISSN: 2783–3518

Review article

Recent Developments in Holographic Black Hole Chemistry

Robert B. Mann
Department of Physics and Astronomy, University of Waterloo, Waterloo, Ontario, N2L 3G1, Canada; and
Perimeter Institute for Theoretical Physics, 31 Caroline St., Waterloo, Ontario, N2L 2Y5, Canada;
E-mail: rbmann@uwaterloo.ca

Received: November 18, 2023; **Revised:** December 13, 2023; **Accepted:** December 20, 2023

Abstract. One of the major developments in classical black hole thermodynamics is the inclusion of vacuum energy in the form of thermodynamic pressure. Known as Black Hole Chemistry, this subdiscipline has led to the realization that anti de Sitter black holes exhibit a broad variety of phase transitions that are essentially the same as those observed in chemical systems. Since the pressure is given in terms of a negative cosmological constant (which parameterizes the vacuum energy), the holographic interpretation of Black Hole Chemistry has remained unclear. In the last few years there has been considerable progress in developing an exact dictionary between the bulk laws of Black Hole Chemistry and the laws of the dual Conformal Field Theory (CFT). Holographic Black Hole Chemistry is now becoming an established subfield, with a full thermodynamic bulk/boundary correspondence, and an emergent understanding of CFT phase behaviour and its correspondence in the bulk. Here I review these developments, highlighting key advances and briefly discussing future prospects for further research.

Keywords: Thermodynamic Holography; Phase Transitions; Black Holes.

Contents

1 Introduction **2**

2 Holographic Smarr Relation **3**

3 Variable G **9**

4 Variable Conformal Factor **10**

5 Holographic Thermodynamics for Charged AdS Black Holes **12**
5.1 Thermodynamic Stability 15
5.2 Fixed $(\tilde{Q}, \mathcal{V}, C)$ 15
5.3 Fixed $(\tilde{\Phi}, \mathcal{V}, C)$ 17
5.4 Fixed $(\tilde{Q}, \mathcal{V}, \mu)$ 19
5.5 Other ensembles and criticality 21

6 Conclusion **22**

1 Introduction

Black Hole Chemistry [1] – an extension of black hole thermodynamics in which the (negative) cosmological constant Λ is identified with a (positive) thermodynamic pressure in d spacetime dimensions via [2, 3, 4, 5, 6]

$$P = -\frac{\Lambda}{8\pi G} = \frac{(d-1)(d-2)}{16\pi L^2 G} \tag{1}$$

– is 15 years old, though its roots extend further back [7, 8, 9]. The introduction of pressure in turn implies a conjugate thermodynamic volume V, and the mass of the black hole can be understood as thermodynamic enthalpy [2]. Incorporation of these quantities into black hole thermodynamics has been shown to yield a range of phenomena as rich as can be found in a chemistry laboratory. Examples include Van der Waals type phase transitions for charged anti de Sitter (AdS) black holes [10], reentrant phase transitions [11, 12], triple points [13, 14, 15], heat engines [16], polymer transitions [17], superfluid transitions [18], Joule-Thompson expansions [19], molecular microstructures [20], and most recently multicritical behaviour [21, 22]. Extensions to asymptotically flat [23], Rindler [24, 25, 26], and de Sitter [27, 28, 29] spacetimes have been carried out in recent years. The formalism can even be extended to solitons [30, 31].

For a charged and multiply-spinning AdS black hole, the generalised Smarr relation and first law are [27]

$$M = \frac{d-2}{d-3}\big(TS + \sum_i \Omega_i J_i\big) + \phi Q - \frac{2}{d-3}PV \tag{2}$$

$$\delta M = T_H \delta S + \phi \delta Q + \sum_i \Omega_i \delta J_i + V \delta P\,, \tag{3}$$

respectively, where M is the mass of the black hole whose angular momenta are J_i. The relative angular velocities Ω_i between the horizon and infinity [32] are their respective thermodynamic conjugates. The remaining thermodynamic variables are the Hawking temperature

T_H, the electric charge Q (with conjugate electrostatic potential ϕ) and the Bekenstein-Hawking entropy S. In general relativity, $S = \frac{A}{4G}$, where the d-dimensional gravitational constant G has the same dimensions as the horizon area A (a length dimension of $(d-2)$), rendering the entropy unitless.

Despite this cornucopia of interesting results, the *holographic interpretation* of black hole chemistry has been somewhat puzzling [16, 33, 34, 35, 36, 37, 38]. Despite the fact that from a cosmological perspective Λ is the energy/pressure of the vacuum, and so might be considered a variable quantity, in the AdS/CFT correspondence [39, 40] Λ is regarded as fixed – it sets the asymptotic structure of the bulk spacetime and is proportional to the number of colours N (or central charge C) in the dual gauge theory. Indeed, an early version of what could be called holographic black hole thermodynamics argued that Anti-de Sitter (AdS) black holes were equivalent to thermal states in the dual conformal field theory (CFT) [41]. Advancing this further, the temperature and entropy of a Schwarzschild-AdS black hole match the respective thermal temperature and entropy of the dual CFT. Furthermore, the first-order phase transition between a large black hole and thermal AdS spacetime (known as the Hawking-Page transition [42]) corresponds to the confinement/deconfinement phase transition of a quark gluon plasma [41]; this transition was later shown to correspond to a liquid-solid transition in black hole chemistry [6].

The holographic dictionary states that the thermodynamics of AdS black holes is completely equivalent to the thermodynamics of the dual CFT. Since a CFT is a standard unitary gauge theory (perhaps with a large number N of color degrees of freedom), the correspondence suggests that black hole evaporation is a unitary process. More generally, one expects that perplexing features of black holes can be studied in the dual field theory, and vice-versa, via holographic duality.

However a variable Λ is difficult to interpret in the context of holographic duality. Its variations correspond to changing both N (or the central charge C) and the CFT volume $\mathcal{V}$ [16, 33, 34, 43]; consequently the first law (3) cannot be straightforwardly related to the corresponding thermodynamics of the dual field theory [44, 45, 46]. Furthermore, electric charge and its conjugate potential both rescale with the AdS length L in the correspondence.

Recently considerable progress has been made in understanding holographic black hole chemistry. An exact dictionary between the laws of Black Hole Chemistry and the laws in the CFT has been constructed. An emergent understanding of CFT phase behaviour and its correspondence in the bulk is taking place, leading to a full thermodynamic bulk/boundary correspondence. In this article I shall review these recent developments, highlighting some key advances and briefly discussing future avenues of research.

2 Holographic Smarr Relation

The general assumption underlying nearly all investigations of the AdS/CFT correspondence is that the cosmological constant is a fixed parameter, related to the number of colours N in the dual gauge theory via a holographic relation of the form [44]

$$\mathsf{k}\frac{L^{d-2}}{16\pi G} = N^2 \tag{4}$$

where the numerical factor k depends on the details of the particular holographic system and L is the AdS length from (1). The relation (4) emerged out of the AdS/CFT correspondence [39], in which the near horizon geometry of N coincident D_3 branes in type IIB supergravity

corresponds to an $AdS_5 \times S^5$ spacetime. Specifically,

$$L^4 = \frac{\sqrt{2}\ell_{Pl}^4}{\pi^2} N \tag{5}$$

where ℓ_{Pl} is the 10-dimensional Planck length, expresses the correspondence with an $\mathcal{N} = 4$ SU(N) Yang-Mills theory on the boundary of the $AdS_5 \times S^5$ spacetime.

These relations suggest that variation of the AdS radius L implies variation of the number of colours N in the corresponding Yang-Mills theory. A consequence of this is that the variation of Λ in the bulk corresponds to variation in the space of field theories in the boundary. There have been a few proposals of this type [16, 33, 34], where V is interpreted in the boundary field theory as an associated chemical potential μ for colour.

An alternative proposal is to keep N fixed. The field theory then remains unchanged, and variation of Λ then corresponds to variation of the curvature radius governing the space on which the field theory is defined [44]. This perspective yields a '*holographic Smarr relation*' based on the scaling properties of the dual field theory. In the limit of large N the free energy $\mathcal{F}$ of the field theory scales as N^2, and so

$$\mathcal{F}(N, \mu, T, l) = N^2 \mathcal{F}_0(\mu, T, l) \tag{6}$$

The equation of state is

$$E = (d-2)p\mathcal{V} \tag{7}$$

for a conformal field theory, and this can be used with (6) to obtain the standard Smarr relation (2) (setting $J = Q = 0$ for simplicity). Recalling (4), varying Λ (or the AdS length L) implies that G must also be varied since N is fixed.

This relation can be extended beyond the large N limit [45]. The bulk correlates of the subleading $1/N$ corrections are related to the couplings in a class of higher curvature generalizations of Einstein gravity known as Lovelock gravity theories. In the context of string theory the additional higher curvature terms in Lovelock gravity are understood as quantum corrections to Einstein gravity. In the context of holographic thermodynamics, the Lovelock couplings are related to a function of N, and their variations dictate the behaviour of the corresponding CFT.

It is instructive to see how this works for the class of charged AdS black holes. The action for Lovelock gravity minimally coupled to electromagnetism ($F_{ab} = \nabla_{[a}A_{b]}$) is

$$I = \frac{1}{16\pi G} \int d^d x \sqrt{-g} \big[\sum_{k=0}^{\frac{d-1}{2}} \hat{\alpha}_{(k)} L^{(k)} - 4\pi G F_{ab} F^{ab} \big]. \tag{8}$$

where $\hat{\alpha}_{(k)}$ is the Lovelock coupling constant for the k-th power of curvature, and

$$L^{(k)} = \frac{1}{2^k} \delta^{a_1 b_1 \ldots a_k b_k}_{c_1 d_1 \ldots c_k d_k} R^{c_1 d_1}_{a_1 b_1} \ldots R^{c_k d_k}_{a_k b_k} \tag{9}$$

is the Euler density of dimension $2k$ composed of powers of the Riemann tensor $R^{c_k d_k}_{a_k b_k}$, with $\delta^{a_1 b_1 \ldots a_k b_k}_{c_1 d_1 \ldots c_k d_k}$ totally antisymmetric in both sets of indices of the Kronecker delta functions. Variation of the metric and gauge field yield the equations of motion

$$\sum_{k=0}^{\frac{d-1}{2}} \hat{\alpha}_{(k)} G^{(k)}{}^a_b = 8\pi G \big[F_{ac} F^c_b - \frac{1}{4} g_{ab} F_{cd} F^{cd} \big] \qquad \nabla_a F^{ab} = 0 \tag{10}$$

where

$$G^{(k)}{}_{b}^{a} = -\frac{1}{2^{k+1}}\delta^{aa_1b_1\ldots a_kb_k}_{bc_1d_1\ldots c_kd_k}R^{c_1d_1}_{a_1b_1}\ldots R^{c_kd_k}_{a_kb_k} \tag{11}$$

each of which independently satisfy

$$\nabla_a G^{(k)}{}_{b}^{a} = 0 \tag{12}$$

which is a generalization of the Bianchi identities.

Imposing spherical symmetry

$$ds^2 = -f(r)dt^2 + f(r)^{-1}dr^2 + r^2 d\Omega^2_{(\kappa)d-2} \qquad F = \frac{Q}{r^{d-2}}dt\wedge dr \tag{13}$$

where $d\Omega^2_{(\kappa)d-2}$ is the line element of a $(d-2)$-dimensional compact space of constant curvature $(d-2)(d-3)\kappa$ ($\kappa = -1, 0, 1$), the equations of motion (10) become [12]

$$\sum_{k=0}^{\frac{d-1}{2}}\alpha_k\left(\frac{\kappa - f}{r^2}\right)^k = \frac{16\pi GM}{(d-2)\omega^{\kappa}_{d-2}r^{d-1}} - \frac{8\pi GQ^2}{(d-2)(d-3)r^{2(d-2)}} \tag{14}$$

where $\omega^{(1)}_{d-2} = \frac{2\pi^{(d-1)/2}}{\Gamma((d-1)/2)}$ and

$$\alpha_0 = \frac{\hat{\alpha}_{(0)}}{(d-1)(d-2)}, \qquad \alpha_1 = \hat{\alpha}_{(1)} \qquad \alpha_k = \hat{\alpha}_{(k)}\prod_{n=3}^{2k}(d-n) \qquad \text{for } k \geq 2 \tag{15}$$

is a useful rescaling of the Lovelock couplings.

Without solving (14), the first law of thermodynamics and the Smarr relation can respectively be shown to be [47]

$$\delta M = T\delta S + \phi\delta Q - \frac{1}{16\pi G}\sum_{k=0}^{\frac{d-1}{2}}\Psi^{(k)}\delta\hat{\alpha}_{(k)} \tag{16}$$

$$(d-3)M = (d-2)TS + (d-3)\phi Q + \sum_{k=0}^{\frac{d-1}{2}}\frac{2(k-1)}{16\pi G}\Psi^{(k)}\hat{\alpha}_{(k)} \tag{17}$$

where

$$\begin{aligned}
M &= \frac{\omega^{(\kappa)}_{d-2}(d-2)}{16\pi G}\sum_{k=0}\alpha_k\kappa^k {r_+}^{d-1-2k} + \frac{\omega^{(\kappa)}_{d-2}Q^2}{2(d-3){r_+}^{d-3}} \\
Q &= \frac{1}{2\omega^{(\kappa)}_{d-2}}\int *F \qquad \phi = \frac{\omega^{(\kappa)}_{d-2}Q}{(d-3)r_+^{d-3}} \\
T &= \frac{1}{4\pi r_+ D(r_+)}\left[\sum_{k=0}\kappa\alpha_k(d-2k-1)(\frac{\kappa}{r_+^2})^{k-1} - \frac{8\pi GQ^2}{(d-2)r_+^{2(d-3)}}\right] \\
S &= \frac{\omega^{(\kappa)}_{d-2}(d-2)}{4G}\sum_{k=0}\frac{k\kappa^{k-1}\alpha_k r_+^{d-2k}}{d-2k} \qquad D(r_+) \equiv \sum_{k=1}k\alpha_k(\kappa r_+^{-2})^{k-1}
\end{aligned} \tag{18}$$

are the respective mass M, charge Q (with conjugate potential ϕ) and (if it is a black hole) temperature T , and entropy S. The quantities

$$\Psi^{(k)} = \frac{\kappa^{k-1}\omega^{(\kappa)}_{d-2}(d-2)}{16\pi G}r_+^{d-2k}\left[\frac{\kappa}{r_+} - \frac{4\pi kT}{d-2k}\right], \qquad k \geq 0 \tag{19}$$

are the thermodynamic conjugates to the $\hat{\alpha}_{(k)}$; both can be regarded as thermodynamic variables [47]. The horizon radius r_+ is the largest root of $f(r) = 0$, and the thermodynamic pressure and volume are given by the $k = 0$ terms

$$P = -\frac{\Lambda}{8\pi G} = \frac{(d-1)(d-2)}{16\pi G}\alpha_0 \qquad V = \omega_{d-2}^{(\kappa)}\frac{r_+^{d-1}}{d-1} \tag{20}$$

so that $P_b V_b = \alpha_0 \Psi^{(0)}$. The CFT volume is $v = \omega_n^{(\kappa)} R^n$ where R is the radius of the sphere on which the CFT is defined. The CFT pressure p has a length dimension of $-(n+1)$.

In Lovelock gravity the free energy does not directly scale with the number of colours N, but rather has the form [44, 45]

$$\mathcal{F}(N, \mu, T, \alpha_j, R) = \sum_{k=0} g_k(N)\mathcal{F}^k(\mu, T, \alpha_j, R) \tag{21}$$

where the $g_k(N)$ are assumed to be polynomial functions, with $g_0(N) = N^2$, where N^2 is the central charge. The thermal properties of AdS black holes can be reinterpreted as those of a CFT at the same finite temperature according to the AdS/CFT correspondence [41], and so

$$\mathcal{F} = M - TS - \phi Q \quad \leftrightarrow \quad \tilde{\mathcal{F}} = \tilde{M} - T\tilde{S} - \tilde{\phi}\tilde{Q} \tag{22}$$

for the grand canonical free energy, where $\tilde{M}, \tilde{S}$, $\tilde{Q} = QL/\sqrt{G}$, $\tilde{\phi} = \phi\sqrt{G}/L$ are the respective mass, entropy, charge, and electrostatic potential per unit volume of the CFT, along with $\alpha_k^F = \alpha_k \left(\frac{L^2}{G}\right)^{(1-k)}$ and $\Psi_F^{(k)} = \Psi^{(k)}\left(\frac{L^2}{G}\right)^{(k-1)}$, with other quantities unchanged.

The grand canonical free energy (21) is a polynomial in $1/N^2$. Only the leading term (of order N^2) in this polynomial is taken into account in Einstein gravity [44], since the large N limit is taken. However additional powers of $1/N^2$ need to be included in the Lovelock case because of contributions from higher curvature terms.

These can be inferred from the dimensionality of the couplings. For some length scale l

$$\alpha_k \sim l^{2(k-1)} \qquad \text{or} \qquad [\alpha_k] = 2(k-1) \tag{23}$$

implying

$$g_k(N) = \beta_k(\alpha_k)^{\frac{d-2}{2(k-1)}} \tag{24}$$

which is

$$N^2 = \beta_0 L^{d-2} = \frac{\delta L^{d-2}}{16\pi G} \tag{25}$$

for $k = 0$, recovering the relationship (4) [44] where δ is an arbitrary dimensionless constant.

For any arbitrary function X of the parameters α_k, (24) implies

$$2(k-1)\alpha_k \frac{\partial X}{\partial \alpha_k} = (d-2) g_k \frac{\partial X}{\partial g_k} \tag{26}$$

for any arbitrary function X of the parameters α_k. Since $-2\alpha_0 \partial_{\alpha_0} = L\partial_L$ (from (1) and (20)), this relation can be written as

$$L\frac{\partial}{\partial L} + \sum_{k=1} 2(k-1)\alpha_k \frac{\partial}{\partial \alpha_k} = (d-2)\sum_{k=0} g_k \frac{\partial}{\partial g_k} \tag{27}$$

after summing over k. In particular

$$2\sum_{k=0}(k-1)\alpha_k\Psi^{(k)} = (d-2)\sum_{k=0} g_k\frac{\partial\mathcal{F}}{\partial g_k} = (d-2)\mathcal{F} \tag{28}$$

using the Euler scaling relation $f(tx_1,\ldots,tx_m) = t^n f(x_1,\ldots,x_m)$ for a homogeneous function of order n, where $\Psi^{(k)} = \frac{\partial\mathcal{F}}{\partial\alpha_k}$ and

$$\mathcal{F} = \sum_{k=0} g_k\frac{\partial\mathcal{F}}{\partial g_k} \tag{29}$$

since $\mathcal{F}$ is an homogeneous function of the g_k of degree 1.

Of course the free energy is not only a function of the g_k, but also depends on R and the charge(s). The derivative of a function $f(l,Z)$ with respect to l is

$$\partial_l f(l,Z)|_{Z_b} = \partial_l f|_Z + z\frac{Z}{l}\partial_Z f|_l. \tag{30}$$

if Z scales as $Z = Z_0 l^z$ for some constant Z_0. For a charged AdS black hole

$$A_b = LA, \quad \phi_b = L\phi, \qquad Q_b = Q/L \qquad R = R_0 L \tag{31}$$

upon converting to a canonical normalized field strength of dimension 2, where A_b is the horizon area. The scaling of R is a consequence of the form

$$ds^2_{boundary} = -dt^2 + L^2 d\Omega^2_{d-2} \tag{32}$$

of the boundary metric [44].

Consequently (28) becomes

$$\begin{aligned}\sum_{k=0} 2(k-1)\alpha_k\Psi^k \qquad &= (d-2)\sum_{k=0} g_k\partial_{g_k}\mathcal{F}\big|_{\phi,T} + R\partial_R\mathcal{F}\big|_{\phi,T,\alpha_{k\geq 1}} + Q\partial_Q\mathcal{F}\big|_{\phi,T,\alpha_k}\\ &= (d-2)\mathcal{F} - M - \phi Q\\ &= (d-3)M - (d-2)TS - (d-3)\phi Q\end{aligned} \tag{33}$$

recovering the bulk Smarr relation (2) upon using (22).

The remaining task is to see how the $g_k(N)$ can be approximated. Since we expect terms for $k \geq 1$ to be suppressed relative to the $k = 0$ case (25), the ansatz

$$g_k(N) \equiv \mathcal{O}(N^{2(1-k)}) \tag{34}$$

will be employed. In the context of higher curvature theories of gravity, the additional contributions can be understood as correction terms to the Einstein-Hilbert action, or in other words, we expect

$$\begin{aligned}&L^{(0)} \sim \mathcal{R}^0 \to N^2 \qquad L^{(1)} \sim \mathcal{R}^1 \to N^0 \qquad L^{(2)} \sim \mathcal{R}^2 \to N^{-2}\\ &\cdots \quad L^{(k)} \sim \mathcal{R}^k \to N^{2(1-k)} \quad \cdots\end{aligned} \tag{35}$$

with $\mathcal{R}$ some scalar measure of the curvature.

These terms make distinct contributions to the scattering amplitude. To illustrate this, consider a field theory coupled to a Yang-Mills gauge theory, whose Lagrangian $L^{(1)}$ gives rise to planar and non planar diagrams. Gauge field self-interaction terms arise from $L^{(1)}$,

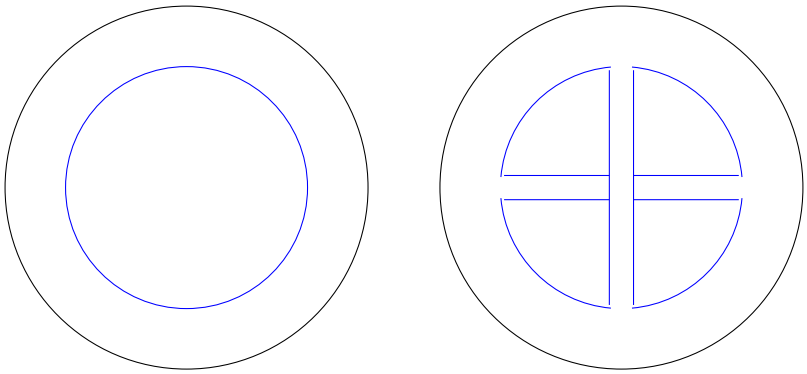

Figure 1: The contribution to the scattering amplitude of the planar diagram on the left is proportional to $N^2(g_{YM})^0 = N^2\lambda^0 = N^2$ and corresponds to $L^{(0)}$ in the Lovelock theory. Contributions to the scattering amplitude from $L^{(1)}$ yield non-planar diagrams of the form shown on the right, and are proportional to $N^2(g_{YM})^4 = N^0\lambda^2 = \lambda^2$. The Yang-Mills coupling g_{YM} appears at each vertex of the diagram. This figure originally appeared in Ref. [45] and is reprinted with permission.

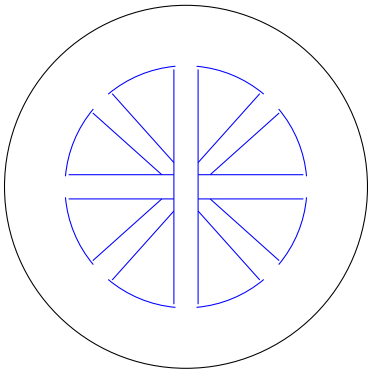

Figure 2: This diagram can be understood as two overlaid copies of the 4-vertex non planar diagram in figure 1. Non-planar diagrams of this form yield contributions to the scattering amplitude proportional to $N^2(g_{YM})^8 = N^{-2}\lambda^4$, and result from $L^{(2)}$ terms in the Lovelock theory. This figure originally appeared in ref. [45] and is reprinted with permission.

whereas higher order diagrams come explicitly from higher curvature terms ($R_{d+1} = R_d + gF^2 + ...$); these will yield non-planar diagrams as shown in figures 1 and 2. Non-planar diagrams with 4 vertices contribute terms proportional to $N^2 g_{YM}^4 = \lambda^2$ – of order N^0 – to the scattering amplitude, where g_{YM} and λ are the respective Yang-Mills and 't Hooft couplings. For $k = 2$ non-planar diagrams of the form shown in figure 2 will contribute terms proportional to $N^2(g_{YM})^8 = N^{-2}\lambda^4$. The $L^{(k)}$ term in the Lovelock action will yield diagrams having a stack of k copies of the four vertices non planar diagram, whose the contribution to the scattering amplitude is proportional to $N^2(g_{YM})^{2k} = N^{2(1-k)}\lambda^{2k}$, commensurate with the correspondence (34). These results are applicable to any higher-curvature theory of gravity.

3 Variable G

One approach in understanding the variation of L whilst retaining the consistency of the relation (4) is to vary the gravitational constant G [48]. This has profound consequences for black hole chemistry and its holographic interpretation.

Recall that the first law is

$$\delta E = T\delta S - pd\mathcal{V} + \tilde{\phi}\delta\tilde{Q} + \Omega\delta J + \tilde{\mu}\delta C\,, \tag{36}$$

for the CFT [46], where p and $\mathcal{V} = \mathcal{V}_0 L^{d-2}$ are the CFT pressure and volume, taking the radius of the sphere on which the CFT is defined to be the AdS length. The quantity E is the CFT energy; it is not the enthalpy. The angular momentum and conjugate angular velocity are respectively J and Ω, and $\tilde{Q}, \tilde{\phi}$ are the respective holographic charge and conjugate potential. The quantity $\tilde{\mu}$ is the chemical potential for the central charge C. For $SU(N)$ gauge theories with conformal symmetry $C \propto N^2$; more generally C is proportional to a power of N.

Dimensionally these quantities scale as

$$[E] \;=\; [T] = [\Omega] = [\tilde{\mu}] = \frac{1}{L} \quad [\mathcal{V}] = L^{d-2} \quad [S] = [\tilde{Q}] = [J] = [C] = L^0 \tag{37}$$

which in turn implies (7) from the standard Euler scaling argument.

Using the fact that $S, \tilde{Q}, J, C$ scale as C, but $\mathcal{V}$ does not [46] yields the *holographic Smarr* relation [46]

$$E = TS + \tilde{\phi}\tilde{Q} + \Omega J + \tilde{\mu}C\,, \tag{38}$$

via a similar Eulerian scaling argument. Note that d-dependent factors are absent in (38) and that no $p - \mathcal{V}$ term appears. Noting the relationship between C and N, equation (4) can be written as

$$C = \mathsf{k}\frac{L^{d-2}}{16\pi G} \tag{39}$$

and furthermore

$$E = M\,, \qquad \tilde{Q} = \frac{QL}{\sqrt{G}}\,, \qquad \tilde{\phi} = \frac{\phi\sqrt{G}}{L}\,, \tag{40}$$

can likewise be identified.

Inserting these relations into (36) yields

$$\begin{aligned} \delta(GM) \;&=\; \tfrac{\kappa}{8\pi}\delta A + \Omega\,\delta(GJ) + \sqrt{G}\phi\,\delta(\sqrt{G}Q) - \tfrac{V}{8\pi}\delta\Lambda \\ \Leftrightarrow \quad \delta M \;&=\; \tfrac{\kappa}{8\pi G}\delta A + \Omega\delta J + \phi\delta Q - \tfrac{V}{8\pi G}\delta\Lambda - \alpha\tfrac{\delta G}{G}\,, \end{aligned} \tag{41}$$

using (1) and (38), where

$$\alpha = \frac{1}{2}\phi Q + \tilde{\mu}C + TS = M - \Omega J - \frac{1}{2}\phi Q\,, \tag{42}$$

$$V = \frac{8\pi G l^2}{(d-1)(d-2)}\Big(M - \phi Q - (d-2)C\tilde{\mu}\Big)$$

$$= \frac{(d-3)}{2P}\Big(\frac{d-2}{d-3}(\Omega J + TS) + \phi Q - M\Big)\,. \tag{43}$$

The last relation is the bulk Smarr relation (2) (with vanishing Lovelock couplings).

Allowing G to vary raises it to the status of a thermodynamic variable, whose conjugate is α/G. When G is held fixed, the first law (41) reduces to (3). Dimensional analysis of the various quantities implies

$$[\phi] = L^{\frac{2-d}{2}}\,, \quad [Q] = L^{\frac{d-4}{2}}\,, \quad [A] = [G] = L^{d-2}\,, \tag{44}$$
$$[M] = \tfrac{1}{L}\,, \quad [\Lambda] = \tfrac{1}{L^2}\,, \quad [P] = \tfrac{1}{L^d}\,, \quad [V] = L^{d-1}\,,$$

and yields the bulk Smarr relation (2) provided (42) holds. Since this relation follows from the holographic Smarr relation, we see a connection between the two.

We can use (39) to write variations of G in terms of C and L (that is, P), and in turn rewrite the bulk first law (41) as

$$\delta M = T\delta S + \Omega\delta J + \phi\delta Q + V_C\delta P + \mu\delta C\,, \tag{45}$$

where

$$V_C = \frac{2M + (d-4)\phi Q}{2dP}\,, \quad \mu = \frac{2P(V_C - V)}{C(d-2)}\,, \tag{46}$$

are a new thermodynamic volume V_C and chemical potential μ.

4 Variable Conformal Factor

The variation of G in the previous section kept the variations of C and $\mathcal{V}$ independent. Since $\mathcal{V} = \mathcal{V}_0 L^{d-2}$, variations of the cosmological constant (the bulk pressure) induce variations of the CFT volume $\mathcal{V}$, and without variation of G, the corresponding CFT first law would be degenerate, since the $\mu\delta C$ and $-p\delta\mathcal{V}$ would not be independent, leaving the CFT interpretation of black hole chemistry obscure at the least. However variation of G as a thermodynamic quantity is likewise fraught with unclear interpretation. For this reason another approach is desirable.

Fortunately such an approach has recently been developed [49]. The boundary metric of the dual CFT is actually [50, 40]

$$ds^2 = \omega^2\Big(-dt^2 + L^2 d\Omega^2_{(\kappa)d-2}\Big) \tag{47}$$

and is obtained by the conformal completion of the bulk AdS spacetime, where ω is an 'arbitrary' dimensionless conformal factor that is a function of boundary coordinates, reflecting the conformal symmetry of the boundary theory.

If ω is set to 1 (the standard choice) than the CFT volume $\mathcal{V} \propto L^{d-2}$, as in the previous section. However we saw in section 2 that in general the radius of the space on which the CFT is defined need not be given in terms of L. This suggests that ω be treated as

a (dimensionless) thermodynamic parameter, rather than a function of the boundary coordinates, making the central charge and volume independent variables. This is not without precedent. For the $\kappa = 0$ planar AdS black brane case, variations of volume $\mathcal{V}$ and central charge C are clearly independent; varying the former corresponds to changing the number of points in the system, whereas varying the latter corresponds to varying the number of degrees of freedom at each point. Since the planar case can be reached as a limit of the $\kappa = 1$ spherical case, it is reasonable to expect this independence to extend to non-planar cases.

Regarding ω as another variable is tantamount to changing the CFT volume, which is now proportional to

$$\mathcal{V} \propto (\omega L)^{d-2} \,. \tag{48}$$

and for Einstein-Maxwell theory implies the following generalized dictionary

$$\begin{aligned} \tilde{S} &= S = \frac{A}{4G} \,, \quad \tilde{E} = \frac{M}{\omega} \,, \quad \tilde{T} = \frac{T}{\omega} \,, \quad \tilde{\Omega} = \frac{\Omega}{\omega} \,, \\ \tilde{J} &= J, \quad \tilde{\Phi} = \frac{\Phi\sqrt{G}}{\omega L} \,, \quad \tilde{Q} = \frac{QL}{\sqrt{G}} \,. \end{aligned} \tag{49}$$

between the bulk (no tildes) and dual CFT (with tildes) thermodynamic quantities. Note that variations in L (or Λ) induce variations in C via (39) with G fixed whilst keeping $\mathcal{V}$ independent, and likewise enter in the variation of spatial volume and electric charge.

Using the Smarr relation (43), the first law (41) (for fixed G) can be rewritten as

$$\begin{aligned} \delta\Big(\frac{M}{\omega}\Big) &= \frac{T}{\omega}\delta\Big(\frac{A}{4G}\Big) + \frac{\Omega}{\omega}\delta J + \frac{\Phi\sqrt{G}}{\omega L}\delta\Big(\frac{QL}{\sqrt{G}}\Big) \\ &+ \Big(\frac{M}{\omega} - \frac{TS}{\omega} - \frac{\Omega J}{\omega} - \frac{\Phi Q}{\omega}\Big)\frac{\delta(L^{d-2}/G)}{L^{d-2}/G} - \frac{M}{\omega(d-2)}\frac{\delta(\omega L)^{d-2}}{(\omega L)^{d-2}}, \end{aligned} \tag{50}$$

which, using (39), (48) and (49), becomes

$$\delta\tilde{E} = \tilde{T}\delta S + \tilde{\Omega}\delta J + \tilde{\Phi}\delta\tilde{Q} + \mu\delta C - p\delta\mathcal{V} \,, \tag{51}$$

which is the CFT first law, where

$$\mu = \frac{1}{C}(\tilde{E} - \tilde{T}S - \tilde{\Omega}J - \tilde{\Phi}\tilde{Q}) \tag{52}$$

$$p = \frac{\tilde{E}}{(d-2)\mathcal{V}} \tag{53}$$

recovering (7) in the latter equation. The duality between the AdS-bulk first law (50) and CFT-boundary first law (51) is now clear.

Eq. (52) is the Euler relation for holographic CFTs. It is dual to the bulk Smarr relation (43) for charged AdS black holes [44, 46]. It follows (on the CFT side) from the proportionality of the thermodynamic quantities with the central charge ($\tilde{E}, \tilde{S}, \tilde{J}, \tilde{Q} \propto C$), and occurs in the deconfined phase (dual to an AdS black hole geometry). Note that (52) has no dimension-dependent factors whereas the bulk Smarr relation (43) does. To see how this works, we can write PV as a partial derivative of the CFT energy $\tilde{E}$

$$-2PV = L\left(\frac{\partial M}{\partial L}\right)_{A,J,Q,G} = L\omega\left(\frac{\partial \tilde{E}}{\partial L}\right)_{A,J,Q,G} \tag{54}$$

and since $\tilde{E} = \tilde{E}(S(A,G), J, \tilde{Q}(Q,L,G), C(L,G), V(L,\omega))$ as a function of bulk quantities, (39), (48) and (49) yield

$$\left(\frac{\partial \tilde{E}}{\partial L}\right)_{A,J,Q,G} = \frac{1}{L}(\tilde{\Phi}\tilde{Q} + (d-2)\mu C - (d-2)p\mathcal{V}) \tag{55}$$
$$= \frac{1}{L}((d-3)(\tilde{E} - \tilde{\Phi}\tilde{Q}) - (d-2)(\tilde{\Omega}J + \tilde{T}S))\,,$$

using (52) and (53). Inserting (55) into (54) yields the bulk Smarr relation (43).

Eq. (53) is the CFT equation of state (7), derivable from CFT scaling symmetry. Note that there is no $p\mathcal{V}$ term in the Euler relation (52), reflecting the fact that the internal energy is not an extensive variable on compact spaces at finite temperature in the deconfined phase. This is a feature of holographic CFTs. For $\omega L\tilde{T} \gg 1$, namely the high-temperature or large-volume regime, the μC term becomes equal to $-p\mathcal{V}$, and the energy becomes extensive.

The rescaling property that yielded the Euler relation and equation of state can be used to eliminate some of the terms in the first law (51). For example the $p\delta V$ term can be removed by rescaling

$$\hat{E} = \omega L\tilde{E} \qquad \hat{T} = \omega L\tilde{T} \qquad \hat{\Omega} = \omega L\tilde{\Omega} \qquad \hat{\Phi} = \omega L\tilde{\Phi} \qquad \hat{\mu} = \omega L\mu \tag{56}$$

yielding

$$\delta\hat{E} = \hat{T}\delta S + \hat{\Omega}\delta J + \hat{\Phi}\delta\tilde{Q} + \hat{\mu}\delta C\,, \tag{57}$$
$$\hat{E} = \hat{T}S + \hat{\Omega}J + \hat{\Phi}\tilde{Q} + \hat{\mu}C\,, \tag{58}$$

from (51) and (52) respectively. Since all thermodynamic quantities are now scale invariant, the thermal description respects the symmetries of the CFT.

Alternatively, the $\mu\delta C$ term can be eliminated from (51) using (52), giving

$$\delta\bar{E} = \tilde{T}\delta\bar{S} + \tilde{\Omega}\delta\bar{J} + \tilde{\Phi}\delta\bar{Q} - \bar{p}\delta\mathcal{V}\,, \tag{59}$$
$$\bar{E} = (d-2)\bar{p}\mathcal{V}\,, \tag{60}$$

with the rescaled quantities:

$$\bar{E} = \frac{\tilde{E}}{C}\,, \quad \bar{S} = \frac{S}{C}\,, \quad \bar{J} = \frac{J}{C}\,, \quad \bar{Q} = \frac{\tilde{Q}}{C}\,, \quad \bar{p} = \frac{p}{C}\,. \tag{61}$$

Note that these barred quantities are no longer proportional to C. All thermodynamic quantities now retain their standard dimensionality, and the 'standard' thermodynamic first law, with $\bar{E}$ interpreted as internal energy, is recovered.

The laws (57) and (58) were recently proposed in another context called the "restricted phase space" approach [51], in which the CFT volume $\mathcal{V}$ is kept fixed and variations in C arise from variations of G in the bulk. The physical interpretation is thus very different and the resultant holographic thermodynamics has nothing to do with the original black hole chemistry. In contrast to the restricted phase space approach, here variation of C (and of $\mathcal{V}$) is induced by variation of Λ in the bulk, with G fixed [49].

5 Holographic Thermodynamics for Charged AdS Black Holes

We can now make use of the preceding considerations to analyze the thermodynamic behaviour of charged AdS black holes from a holographic viewpoint [52]. There are three pairs

of conjugate quantities – $(\tilde{\Phi}, \tilde{Q})$, $(p, \mathcal{V})$ and (μ, C) – and so there are eight possible thermodynamic (grand) canonical ensembles in the CFT. Only three of these – fixed $(\tilde{Q}, \mathcal{V}, C)$, fixed $(\tilde{\Phi}, \mathcal{V}, C)$, and fixed $(\tilde{Q}, \mathcal{V}, \mu)$ – exhibit interesting phase behaviour or critical phenomena [52].

The action for electromagnetism minimally coupled to Einstein gravity is given by (8) with $\alpha_{(k)} = 0$ for $k \geq 2$. For later convenience we write this as

$$I = \frac{1}{16\pi G} \int d^d x \sqrt{-g} \left(R - 2\Lambda - F^2 \right) \tag{62}$$

in d spacetime dimensions, with Λ is given in (1). Note the normalisation $1/16\pi G$ of the matter action, which is not standard.

The field equations yield the solution

$$ds^2 = -f(r) dt^2 + \frac{dr^2}{f(r)} + r^2 d\Omega_{d-2}^2 \tag{63}$$

in the spherically symmetric case, where

$$f(r) = 1 + \frac{r^2}{L^2} - \frac{m}{r^{d-3}} + \frac{q^2}{r^{2d-6}} \,. \tag{64}$$

and m is the mass parameter of the black hole. It is related to the ADM mass by

$$M = \frac{(d-2)\Omega_{d-2}}{16\pi G} m \tag{65}$$

where Ω_{d-2} is area of the unit $d-2$ round sphere. The associated gauge potential is

$$A = \left(-\frac{1}{\zeta} \frac{q}{r^{d-3}} + \Phi \right) dt \tag{66}$$

and the electric charge is related to the charge parameter q via

$$Q = \frac{(d-2)\Omega_{d-2}}{8\pi G} \zeta \, q \,, \qquad with \qquad \zeta = \sqrt{\frac{2(d-3)}{d-2}} \tag{67}$$

where Φ is a constant that plays the role of the electric potential.

Since $f(r_h) = 0$ where r_h is the (outer) horizon radius, we can write

$$m = r_h^{d-3} \left(1 + \frac{r_h^2}{L^2} + \frac{q^2}{r_h^{2d-6}} \right) \tag{68}$$

and

$$\Phi = \frac{1}{\zeta} \frac{q}{r_h^{d-3}} \tag{69}$$

by requiring $A_t(r_h) = 0$. This choice implies that Φ is the potential difference between the outer horizon and infinity. The Hawking temperature T and the Bekenstein–Hawking entropy S are

$$T = \frac{d-3}{4\pi r_h} \left(1 + \frac{d-1}{d-3} \frac{r_h^2}{L^2} - \frac{q^2}{r_h^{2d-6}} \right) \qquad S = \frac{\Omega_{d-2} r_h^{d-2}}{4G} \tag{70}$$

which can be obtained by computing the surface gravity defined with respect to the time translation Killing vector $\xi = \partial_t$ and the horizon area respectively.

It is straightforward to show that the thermodynamic quantities (65), (67), (69), and (70) obey the Smarr relation (43) and first law

$$dM = TdS + \Phi dQ - \frac{V}{8\pi G_N} d\Lambda - (M - \Phi Q)\frac{dG}{G} \tag{71}$$

whose latter term differs from that in (41) due to the choice of normalization in the matter part of the action (62). The effect of this is to redefine the bulk charge and potential as $Q_b \to \sqrt{G}Q$ and $\Phi_b \to \Phi/\sqrt{G}$, where Q_b and Φ_b denote the charge and potential in previous sections, yielding $\Phi dQ + \Phi Q dG/G = \Phi_b dQ_b + \frac{1}{2}\Phi_b Q_b dG/G$, whose insertion into (71) recovers (41).

The considerations of the previous section indicate that from (48) we can choose the spatial volume of the CFT to be

$$\mathcal{V} = \Omega_{d-2} R^{d-2} \tag{72}$$

by taking the boundary curvature radius R to differ from L. $\mathcal{V}$ is the volume of a $(d-2)$-dimensional sphere of radius R in the CFT boundary geometry $\mathbb{R} \times S^{d-2}$, which corresponds to an "area" in the d-dimensional AdS bulk geometry. Asymptotically,

$$ds^2 = -\frac{r^2}{L^2}dt^2 + \frac{L^2}{r^2}dr^2 + r^2 d\Omega_{d-2}^2 \to ds^2 = -\frac{R^2}{L^2}dt^2 + R^2 d\Omega_{d-2}^2 \tag{73}$$

by choosing the Weyl factor relating the AdS and CFT metrics to be $\lambda = R/r$. The holographic dictionary is then [44, 46, 53]

$$S = \frac{A}{4G_N}\,, \qquad E = M\frac{L}{R}\,, \qquad T = \frac{\kappa}{2\pi}\frac{L}{R}\,, \qquad \tilde{\Phi} = \frac{\Phi}{L}\frac{L}{R}\,, \qquad \tilde{Q} = QL\,. \tag{74}$$

for this choice of CFT metric. The L/R factor appears because the bulk Schwarzschild time t differs from the boundary CFT time in (73) by a factor R/L [54]. The holographic dictionary (72) and (74) then implies (setting $J = 0$) the first law (36) along with the Smarr relation (52) and equation of state (53) for the CFT.

In analyzing the phase behaviour in the CFT, it is useful to write [37]

$$x \equiv \frac{r_h}{L}\,, \qquad y \equiv \frac{q}{L^{d-2}}\,. \tag{75}$$

upon which (65), (70), and (74) become

$$E = \frac{d-1}{R} C x^{d-2}\left(1 + x^2 + \frac{y^2}{x^{2d-4}}\right) \qquad T = \frac{d-2}{4\pi R}\frac{1}{x}\left(1 + \frac{d}{d-2}x^2 - \frac{y^2}{x^{2d-4}}\right) \tag{76}$$

$$S = 4\pi C x^{d-1} \qquad \tilde{Q} = 2\alpha(d-1)Cy \qquad \tilde{\Phi} = \frac{1}{\alpha R}\frac{y}{x^{d-2}} \tag{77}$$

and we obtain

$$\mu = \frac{x^{d-2}}{R}\left(1 - x^2 - \frac{y^2}{x^{2d-4}}\right) \tag{78}$$

for (52).

5.1 Thermodynamic Stability

In analyzing various ensembles, the key quantity of interest is the free energy. The expression for the free energy (or thermodynamic potential) depends on the choice of ensemble, but in all cases the equilibrium state corresponds to its global minimum. The state yielding the global minimum of the free energy is generally the thermodynamically stable state.

The sign of the specific heat (or heat capacity)

$$C_P \equiv C_{P,J_1,\ldots,J_N,Q_1,\ldots,Q_n} = T\Big(\frac{\partial S}{\partial T}\Big)_{P,J_1,\ldots,J_N,Q_1,\ldots,Q_n} \tag{79}$$

provides information about local thermodynamic stability; if $C_P > 0$ then a given state is locally thermodynamically stable, though it may not be the most stable thermodynamic state. Considering the free energy as a function of temperature, locally stable states are those for which the 2nd derivative is negative, whereas locally unstable states have positive 2nd derivative.

In what follows we shall find thermodynamically stable and unstable phases for the various ensembles, commenting on these in turn.

5.2 Fixed $(\tilde{Q}, \mathcal{V}, C)$

Fixing the charge $\tilde{Q}$, spatial volume $\mathcal{V}$ and central charge C corresponds to the canonical ensemble, whose thermodynamic potential $\mathrm{F} \equiv E - TS = C\frac{x^{d-2}}{R}\left(1 - x^2 + (2d-3)\frac{y^2}{x^{2d-4}}\right)$ is the Helmholtz free energy. Since

$$d\mathcal{F} = dE - TdS - SdT = -SdT + \tilde{\Phi}d\tilde{Q} - pd\mathcal{V} + \mu dC \tag{80}$$

$\mathcal{F}$ is stationary at fixed $(T, \tilde{Q}, \mathcal{V}, C)$.

To understand phase behaviour, we wish to plot $\mathcal{F}$ as a function of T, which can both be regarded as functions of $(\tilde{Q}, R, C, x)$; from (72), fixing R is equivalent to fixing $\mathcal{V}$. Using (77) to eliminate y yields

$$\begin{aligned} \mathcal{F} &= C\frac{x^{d-2}}{R}\left(1 - x^2 + \frac{2d-3}{4\alpha^2(d-1)^2C^2}\frac{\tilde{Q}^2}{x^{2d-4}}\right), \\ T &= \frac{d-2}{4\pi R}\frac{1}{x}\left(1 + \frac{d}{d-2}x^2 - \frac{2d-3}{4\alpha^2(d-1)^2C^2}\frac{\tilde{Q}^2}{x^{2d-4}}\right). \end{aligned} \tag{81}$$

and plotting $\mathcal{F}$ in terms of T is straightforward. Note that dependence on R is trivially fixed by scale invariance and so $R = 1$ can be taken without loss of generality.

The results are illustrated in Fig. 3 for a variety of choices of $\tilde{Q}$ relative to fixed C (up) and of C relative to fixed $\tilde{Q}$ (down). In both cases the free energy displays "swallowtail" behaviour connecting three different branches, but in the former case this only occurs for $\tilde{Q} < \tilde{Q}_{crit}$ and in the latter case for $C > C_{crit}$, where $\tilde{Q}_{crit}$ and C_{crit} are critical values whose ratio is [52]

$$\frac{C_{crit}}{\tilde{Q}_{crit}} = \frac{1}{2\alpha(d-1)y_{crit}} = \sqrt{\frac{(2d-3)}{8(d-2)}}\frac{1}{x_{crit}^{d-2}}. \tag{82}$$

In Fig. 3 the former case is shown on the upper plot and the latter case is shown on the lower plot.

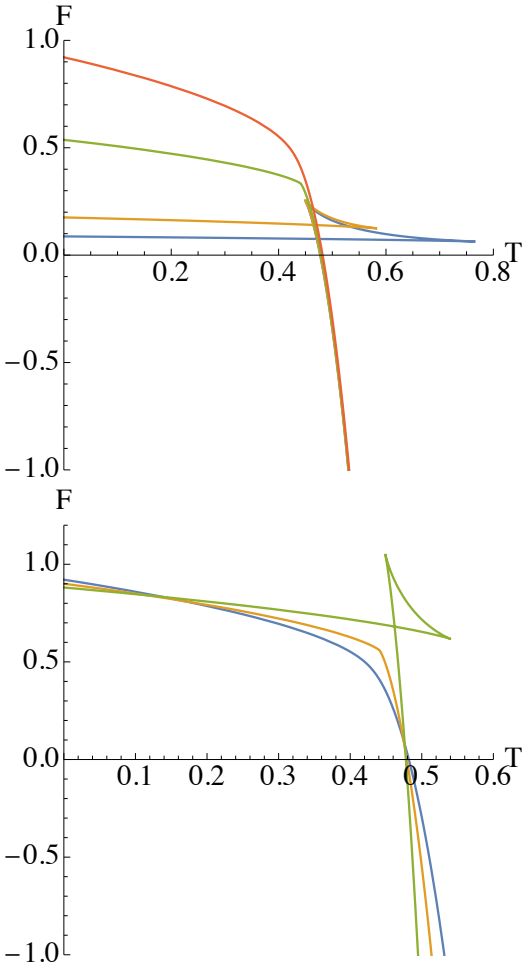

Figure 3: Free energy $\mathcal{F}$ vs. temperature T plot in $d = 4$ for fixed $(\tilde{Q}, \mathcal{V}, C)$, setting $R = 1$. **Up**: Plots for fixed $C = 1$ for $\tilde{Q} = 0.1, 0.2, 4/3\sqrt{5}, 1$ (blue, orange, green, red). First-order phase transitions occur for $\tilde{Q} < \tilde{Q}_{crit}$ (blue, orange) as the "swallowtail" structure indicates, whereas there is a second-order phase transition for $\tilde{Q} = \tilde{Q}_{crit}$ (green). No phase transitions occur for $\tilde{Q} > \tilde{Q}_{crit}$ (red). **Down**: Plots for fixed $\tilde{Q} = 1$ for $C = 1, 3\sqrt{5}/4, 4$ (blue, orange, green). There is a critical central charge above which a swallowtail is present (green) and there is a first-order phase transition. For $C < C_{crit}$ (blue) no phase transitions take place, and for $C = C_{crit}$ (orange) there is a second order phase transition. The apparent triple intersections of the blue, orange and green curves is a consequence of plotting resolution. This figure originally appeared in ref. [52].

We see the appearance of a both a critical electric charge (upper panel) and a critical central charge (lower panel). If C is fixed, for $\tilde{Q} > \tilde{Q}_{crit}$ there are no phase transitions, whereas for $\tilde{Q} < \tilde{Q}_{crit}$ a swallowtail appears, indicating a first-order phase transition. Since the CFT entropy $S = 4\pi C x^{d-1}$, small AdS charged black holes are dual to CFT thermal states with small S/C, namely states with low entropy per degree of freedom. Such states occur for low temperatures and have the smallest $\mathcal{F}$. As T increases, the self-intersection point of the curve is eventually reached, and there is then a transition to a CFT state of high entropy (per degree of freedom), corresponding to large AdS black holes. These states now have the lowest free energy and are along the steep (near-vertical) branch of the curve. As $\tilde{Q}$ increases, the phase transition occurs at larger values of T, whilst the swallowtail shrinks in size, vanishing at $\tilde{Q} = \tilde{Q}_{crit}$, at which point the phase transition becomes second order. This behaviour is commensurate with the canonical ensemble for AdS black holes at fixed charge [10, 53]; the critical point $(\tilde{Q}_{crit}, T_{crit})$ depends on the value of C.

There is likewise for any fixed $\tilde{Q}$ a critical value of C *above* which there is a first order phase transition, as shown in the right panel of figure 3 [48]. For $C > C_{crit}$ the transition is again between states with low- and high-entropy per degree of freedom, and at at C_{crit} there is a second-order phase transition; a single phase is present for $C < C_{crit}$. As C decreases the value of $\mathcal{F}$ at which the first-order phase transition occurs also decreases whereas for fixed C, $\mathcal{F}$ increases as $\tilde{Q}$ decreases.

5.3 Fixed $(\tilde{\Phi}, \mathcal{V}, C)$

Fixing the potential $\tilde{\Phi}$, instead of the charge $\tilde{Q}$, yields

$$\mathcal{W} \equiv E - TS - \tilde{\Phi}\tilde{Q} = \mu C = C\frac{x^{d-2}}{R}\left(1 - x^2 - \frac{y^2}{x^{2d-4}}\right) \tag{83}$$

for the thermodynamic potential of this ensemble, which is the Gibbs free energy. The middle equation follows from (52), and so the free energy $\mathcal{W} \propto \mu$. The last equality follows from (78).

Writing $\tilde{\Phi} = y/\alpha R x^{d-2}$ yields

$$\mathcal{W} = C\frac{x^{d-2}}{R}\left(1 - x^2 - \alpha^2 R^2 \tilde{\Phi}^2\right) \qquad T = \frac{d-2}{4\pi R}\frac{1}{x}\left(1 + \frac{d}{d-2}x^2 - \alpha^2 R^2 \tilde{\Phi}^2\right) \tag{84}$$

allowing a parametric plot of $\mathcal{W}(T)$ using x as parameter, shown in Fig. 4.

In this case at $\mathcal{W} = 0$ there is a first-order phase transition between the high-entropy "deconfined" state and a "confined" state. This is dual to a generalised Hawking-Page transition between a large black hole and thermal AdS, depending on the value of $\tilde{\Phi}$. Setting $\mathcal{W} = 0$ and eliminating x in terms of T yields

$$\tilde{\Phi} \;\; = \tfrac{\tilde{\Phi}_c}{T_c}\sqrt{T_c^2 - T^2}\,, \qquad with \qquad T_c = \tfrac{d-1}{2\pi R}\,, \qquad \tilde{\Phi}_c = \tfrac{1}{\alpha R} = \tfrac{1}{R}\sqrt{\tfrac{d-1}{2d-4}} \tag{85}$$

which describes the coexistence line between the two phases shown in the lower panel of figure 4. At $T = 0$ the phase transition occurs at $\tilde{\Phi} = \tilde{\Phi}_c$, and at $\tilde{\Phi} = 0$ the transition is at $T = T_c$, and is equivalent to the standard Hawking-Page phase transition in the bulk.

For $\tilde{\Phi} < \tilde{\Phi}_c$ (blue curve in the upper panel of figure 4) the free energy curve is a cusp. The upper branch corresponds to low-entropy CFT states (dual to small black holes) whereas the lower branch corresponds to high-entropy CFT states (dual to large black holes). The

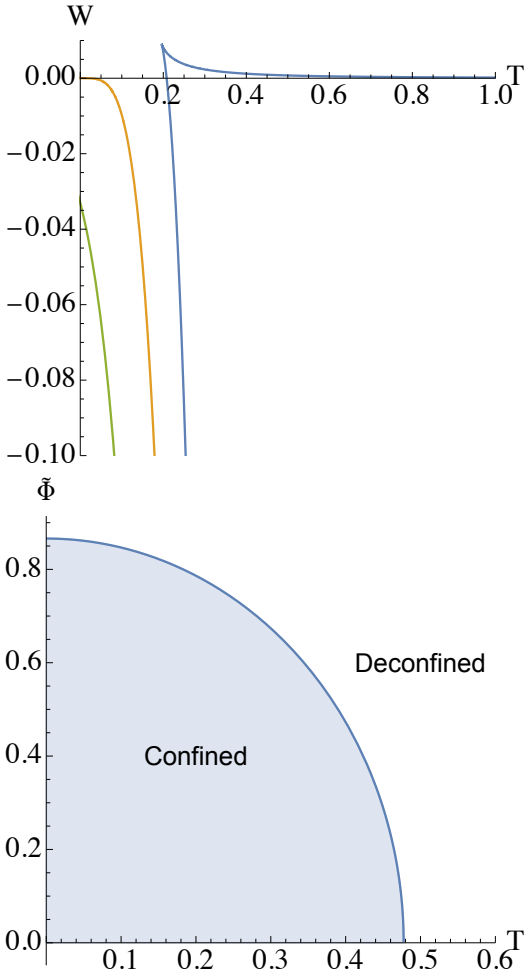

Figure 4: Free energy $\mathcal{W}$ vs. temperature T plot and phase diagrams in $d = 4$ for fixed $(\tilde{\Phi}, \mathcal{V}, C)$, setting $R = 1$. **Up**: Plots for the parameters $C = 1$ and $\tilde{\Phi} = 0.9\Phi_c$ (blue), $\tilde{\Phi} = \Phi_c = \sqrt{3}/2$ (orange) and $\tilde{\Phi} = 1.1\Phi_c$ (green). For $\tilde{\Phi} < \Phi_c$ the free energy curve is two branches joining in a cusp, with the upper/lower branches corresponding to a low/high-entropy states. Now there is a first-order phase transition at $\mathcal{W} = 0$ between the high-entropy "deconfined" state and a "confined" state, dual to a generalised Hawking-Page transition between a large black hole and thermal AdS, depending on the value of $\tilde{\Phi}$. For $\Phi \geq \Phi_c$ the curve never has $\mathcal{W} > 0$ and so no phase transition occurs. **Down**: Phase diagram for $C = 1$; the coexistence curve is a line of (de)confinement phase transitions in the CFT. At $T = 0$ the transition takes place at $\tilde{\Phi} = \tilde{\Phi}_c$ whereas it occurs at the Hawking-Page temperature $T = T_c = 3/2\pi$ for $\tilde{\Phi} = 0$. This figure originally appeared in ref. [52].

temperature as a function of x is minimized at the cusp

$$\left(\frac{\partial T}{\partial x}\right)_{\tilde{\Phi}} = 0 \quad at \quad x_{cusp} = \sqrt{\frac{d-2}{d}(1-\alpha^2 R^2 \tilde{\Phi}^2)}\,, \Rightarrow \qquad T_{cusp} = \frac{1}{2\pi R}\sqrt{d(d-2)(1-\alpha^2 R^2 \tilde{\Phi}^2)} \tag{86}$$

which is turn is the coldest possible (unstable) deconfined state. The specific heat is positive/negative on the lower/upper branch indicative of stable/unstable solutions.

5.4 Fixed ($\tilde{Q}$, $\mathcal{V}$, μ)

For fixed chemical potential μ, the free energy is

$$\mathcal{G} \equiv E - TS - \mu C = \tilde{\Phi}\tilde{Q} \tag{87}$$

where (52) was used to obtain the last equality. The differential of $\mathcal{G}$ is

$$d\mathcal{G} = -SdT + \tilde{\Phi}d\tilde{Q} - pd\mathcal{V} - Cd\mu \tag{88}$$

using the first law (36), and so $\mathcal{G}$ is stationary at fixed $(T, \tilde{Q}, \mathcal{V}, \mu)$.

Although fixing the chemical potential instead of the number of degrees of freedom is very natural in thermodynamics, this ensemble has only recently been considered [52]. Here fixed μ implies that the central charge can vary, which is only possible if we consider a family of holographic CFTs having different central charges. In the gravity theory this corresponds to allowing for variations of Λ (and $\mathcal{G}$).

Using (78) and (77) gives

$$\mathcal{G} \quad = \tfrac{|\tilde{Q}|}{\alpha R}\sqrt{1 - x^2 - \tfrac{R\mu}{x^{d-2}}}\,, \tag{89}$$

$$T \quad = \tfrac{d-2}{4\pi R}\left(\tfrac{R\mu}{x^{d-1}} + \tfrac{2(d-1)}{d-2}x\right)\,. \tag{90}$$

where (87) implies that

$$\mathcal{G} = \frac{L}{R}\Phi Q = \frac{L}{R}\frac{(d-1)\Omega_{d-1}}{8\pi G}\frac{q^2}{r_h^{d-2}} \geq 0$$

which is why the absolute value of $\tilde{Q}$ appears in (89).

In figure 5 a plot of $\mathcal{G}(T)$ is given for several values of μ, along with the phase diagram for this ensemble. For $0 < \mu < \mu_{coin}$ (red and purple curves) there are two branches, cutting the $\mathcal{G} = 0$ line at two temperatures

$$T_1 = \frac{3 - 4\mu R + 3\sqrt{1-4\mu R}}{\sqrt{2}\pi R\left(1+\sqrt{1-4\mu R}\right)^{3/2}}\,, \qquad T_2 = \frac{3 - 4\mu R - 3\sqrt{1-4\mu R}}{\sqrt{2}\pi R\left(1-\sqrt{1-4\mu R}\right)^{3/2}} \tag{91}$$

for $d = 4$, with $T_2 \geq T_1$. For any value of d the two intersection points correspond to the two positive roots of the function $f(x) = 1 - x^2 - \frac{R\mu}{x^{d-2}}$ in (89). The lower branch is a high-entropy state, and is thermodynamically preferred for $T_0 < T < T_1$, where

$$T_0 = \frac{d}{2\pi R}\left(\frac{d-2}{2}\mu R\right)^{1/d} \tag{92}$$

is the temperature at the cusp, obtained from solving $\frac{\partial T}{\partial x}|_{\mu} = 0$. For larger values of T this phase does not exist, and the CFT undergoes a zeroth-order phase transition to the

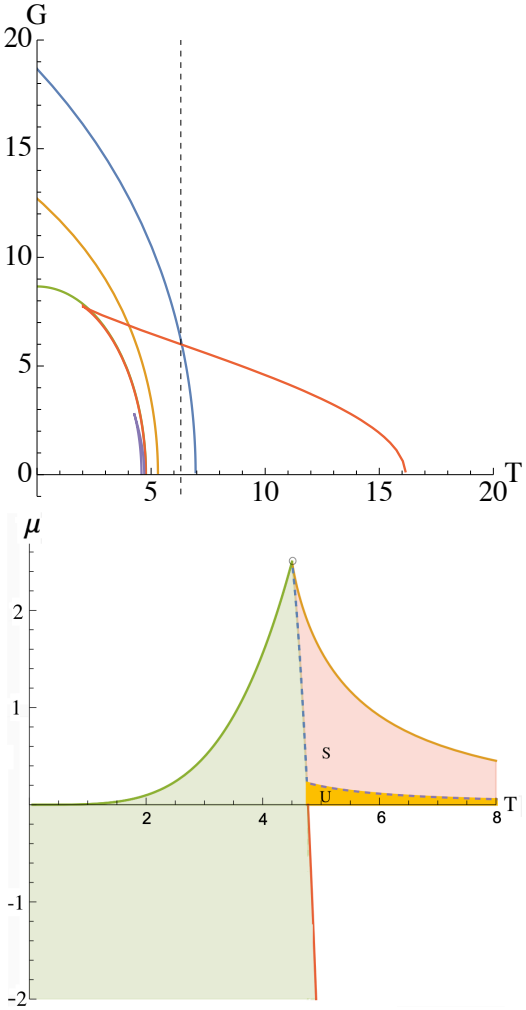

Figure 5: Free energy $\mathcal{G}$ vs. temperature T plot and phase diagram for fixed $(\tilde{Q}, \mathcal{V}, \mu)$ for $R = 0.1$ and $\tilde{Q} = 1$ in $d = 4$. **Up**: Free energy $\mathcal{G}(T)$ for $\mu = -60, -10, 0, 1/10, 2$ (blue, orange, green, red, purple curves). We see the existence of a single stable phase for $\mu \leq 0$ (blue, orange, green curves). There are branches for $\mu > 0$ (red, purple curves) that meet at a cusp $T = T_0$ (92), corresponding to two CFT phases. These branches meet the $\mathcal{G} = 0$ line at the temperatures $T_1 \leq T_2$ (91). The upper/lower branch corresponds to a low/high entropy state. The specific heat is positive along the upper branch near and below $T = T_2$, but becomes negative at some intermediate temperature T_{int}, indicated by the black dashed line for the red curve. Nevertheless, this phase is the thermodynamically preferred phase for $T > T - 1$. Once $T = T_1$, there is a a zeroth-order phase transition to the high-entropy CFT phase given by the lower branch. As T further decreases this phase is preferred, until $T = T_0$ at which point both phases coincide. Below this temperature there are no CFT states. **Down**: The $\mu - T$ phase diagram indicating the different phases. High-entropy phases are in the green shaded region bounded by the green curve. Here the heat capacity is positive. The orange and red regions on the right above the T-axis correspond respectively to stable ("S") and unstable ("U") low-entropy phases having respective positive and negative heat capacities. White regions indicate that no solution exists. This figure originally appeared in ref. [52].

low-entropy CFT phase on the upper branch. This branch has positive specific heat near and below $T = T_2$, but becomes negative at some intermediate temperature

$$T_{int} = \frac{(d-2)\mu\left(\frac{2}{d\mu R}\right)^{\frac{d-1}{d-2}}}{4\pi} + \frac{(d-1)\left(\frac{2}{d\mu R}\right)^{-\frac{1}{d-2}}}{2\pi R}, \tag{93}$$

indicated (for the red curve) by the black dashed line in the upper panel of figure 5. For $T_{int} > T > T_0$ the low-entropy phase has negative heat capacity and so is unstable for these low temperatures. The temperatures T_{int} and T_1, at which the zeroth-order phase transition occurs, coincide for two values of the chemical potential. One is at $\mu = \mu_*$, which is at

$$\mu_* = \frac{1}{324R}\left(16\sqrt{7} - 35\right) \qquad T_* = \frac{2}{3\pi R}\sqrt{2 + 8/\sqrt{7}} \tag{94}$$

for $d = 4$. This means that for $0 < \mu < \mu_*$ the phase transition happens between the *unstable* low-entropy state and the stable high-entropy state. For larger values of μ the zeroth-order phase transition takes place between the *stable* low-entropy phase and the high-entropy phase. This occurs in the region $\mu_* < \mu < \mu_{coin}$, where $\mu_{coin} = \frac{2}{dR}\left(\frac{d-2}{d}\right)^{\frac{d-2}{2}}$ is the value of μ at which $T_2 = T_1 = T_{coin} = \frac{\sqrt{d(d-2)}}{2\pi R} = T_0(\mu_{coin})$. The free energy is not real for $\mu > \mu_{coin}$, and no CFT phases exist for these values of μ.

As μ decreases, T_2 becomes increasingly large and T_1 decreases. For $\mu = 0$, $T_2 \to \infty$ and $T_1 = \frac{3}{2\pi R}$. A qualitative change takes place at $\mu = 0$ (green curve) – the free energy curve becomes single-valued (and monotonically decreasing). This persists for all values of $\mu < 0$ (blue, orange curves). The single-valuedness indicates a single phase in the CFT.

Although the zeroth-order phase transition can take place as temperature increases above T_1, such a transition has the peculiar feature that the entropy decreases during the process, in contradiction to the second law of thermodynamics. The phase transition from the low-entropy to the high-entropy state happens for T decreasing below $T = T_1$, increasing the entropy during the process. Such a transition seems more favourable thermodynamically.

The phase diagram in the lower panel of figure 5 shows the high-entropy phase in green and the low-entropy phase in red (for the stable region having positive heat capacity) and orange (for the unstable region with negative heat capacity). The coexistence curve between the high and low entropy phases is the boundary between the green region and the red/orange one. There are no solutions in the white regions. The boundary of the green high entropy region is determined by T_1 and is indicated by the red line. The right and left boundaries for $\mu > 0$ are respectively set by T_2 and T_0; these meet at the coincidence point, $\mu = \mu_{coin}$. The boundary between the red (stable) and orange (unstable) low-entropy phases is set by T_{int}. The two coexistence lines (the intersection of the two dashed lines) meet at the point (μ_*, T_*).

5.5 Other ensembles and criticality

Critical points in the $\tilde{Q} - \tilde{\Phi}$ and $C - \mu$ planes can both be shown to have mean field critical exponents. In the former case criticality has been observed [37] but the latter case is a genuinely novel recent discovery [52]. None of the other five ensembles display critical phenomena or phase transitions, though some ensembles have two different branches corresponding to low and high entropy phases [52].

6 Conclusion

Holographic Black Hole Chemistry is now on a considerably firmer footing than it was a few years ago. The duality between the first laws in the AdS bulk (50) and dual CFT (51) is now clear, as is the duality between the bulk Smarr relation (43) and the CFT Smarr relation (52). The stage is set to obtain a new and deeper understanding of gauge-gravity duality from a thermodynamic perspective.

One possible line of research is to better understand going beyond the large-N limit. This has been done to some extent for the holographic Smarr relation in section 2 [45]. However in $SU(N)$ gauge theories with conformal symmetry such as $\mathcal{N} = 4$ supersymmetric Yang-Mills theory, the central charge $C \sim N^2$. Changing the rank N of the gauge group is tantamount to changing the original theory, and so variations of C can be regarded as moving within the space of theories and changing the number of degrees of freedom N^2. But this cannot be done continuously since N is an integer. In the large-N limit, $\Delta N/N \ll 1$, and hence $\mu dC \sim dC/C \ll 1$, which makes sense in this limit. However subleading terms are induced by higher curvature corrections, as pointed out in section 2, and understanding the variation of C in this case merits further study.

There have also been recent studies on rotating AdS black holes [55, 56] where, as for charged black holes, the (inverse) central charge plays a role similar to that of thermodynamic pressure. There are 8 possible ensembles, all of which have classical superradiant instabilities in the bulk; what this means for the CFT remains to be understood. Other studies are emerging, including an investigation of the topological properties of bulk/boundary phase transitions [57], and understanding the holographic CFT of accelerating black holes [58]. Recent work on holographic complexity has shown that the the complexity of formation scales with bulk thermodynamic volume (and not entropy) for large black holes, something particularly manifest for rotating black holes [59, 60, 61, 62].

These results but are a small sample of what lies ahead. The holographic implications for the full panoply of results in Black Hole Chemistry [1] remain to be explored!

Data Availability

The manuscript has no associated data or the data will not be deposited.

Conflicts of Interest

The author declares that there is no conflict of interest.

Ethical Considerations

The author has diligently addressed ethical concerns, such as informed consent, plagiarism, data fabrication, misconduct, falsification, double publication, redundancy, submission, and other related matters.

Acknowledgment

This work was supported in part by the Natural Sciences and Engineering Research Council of Canada. I am grateful to Moaathe Belhaj Ahmed, Wan Cong, David Kubiznak, Cedric Sinamuli, and Manus Visser for their collaborations that led to the results presented here.

References

[1] D. Kubiznak, R. B. Mann, and M. Teo, "Black hole chemistry: thermodynamics with Lambda", Class. Quant. Grav. **34** 6 063001 (2017). DOI: 10.1088/1361-6382/aa5c69

[2] D. Kastor, S. Ray, and J. Traschen, "Enthalpy and the Mechanics of AdS Black Holes", Class. Quant. Grav. **26**, 195011 (2009). DOI: 10.1088/0264-9381/26/19/195011

[3] B. P. Dolan, "Pressure and volume in the first law of black hole thermodynamics", Class. Quant. Grav. **28**, 235017 (2011). DOI: 10.1088/0264-9381/28/23/235017

[4] B. P. Dolan, "The cosmological constant and the black hole equation of state", Class. Quant. Grav. **28**, 125020 (2011). DOI: 10.1088/0264-9381/28/12/125020

[5] M. Cvetic, G. W. Gibbons, D. Kubiznak, and C. N. Pope, "Black Hole Enthalpy and an Entropy Inequality for the Thermodynamic Volume", Phys. Rev. D **84**, 024037 (2011). DOI: 10.1103/PhysRevD.84.024037

[6] D. Kubiznak and R. B. Mann, "Black hole chemistry", Can. J. Phys. **93**, 9 999–1002 (2015). DOI: 10.1139/cjp-2014-0465

[7] C. Teitelboim, "The cosmological constant as a thermodynamic black hole parameter", Phys. Lett. B **158**, 293–297 (1985). DOI: 10.1016/0370-2693(85)91186-4

[8] J. D. E. Creighton and R. B. Mann, "Quasilocal thermodynamics of dilaton gravity coupled to gauge fields", Phys. Rev. D **52**, 4569–4587 (1995). DOI: 10.1103/PhysRevD.52.4569

[9] M. M. Caldarelli, G. Cognola, and D. Klemm, "Thermodynamics of Kerr-Newman-AdS black holes and conformal field theories", Class. Quant. Grav. **17**, 399–420 (2000). DOI: 10.1088/0264-9381/17/2/310

[10] D. Kubiznak and R. B. Mann, "P-V criticality of charged AdS black holes", JHEP **07**, 033 (2012). DOI: 10.1007/JHEP07(2012)033

[11] N. Altamirano, D. Kubiznak, and R. B. Mann, "Reentrant phase transitions in rotating anti–de Sitter black holes", Phys. Rev. D **88**, 10 101502 (2013). DOI: 10.1103/PhysRevD.88.101502

[12] A. M. Frassino, D. Kubiznak, R. B. Mann, and F. Simovic, "Multiple Reentrant Phase Transitions and Triple Points in Lovelock Thermodynamics", JHEP **09**, 080 (2014). DOI: 10.1007/JHEP09(2014)080

[13] N. Altamirano, D. Kubiznak, R. B. Mann, and Z. Sherkatghanad, "Kerr-AdS analogue of triple point and solid/liquid/gas phase transition", Class. Quant. Grav. **31**, 042001 (2014). DOI: 10.1088/0264-9381/31/4/042001

[14] S.-W. Wei and Y.-X. Liu, "Triple points and phase diagrams in the extended phase space of charged Gauss-Bonnet black holes in AdS space", Phys. Rev. D **90**, 4 044057 (2014). DOI: 10.1103/PhysRevD.90.044057

[15] A. Dehghani, S. H. Hendi, and R. B. Mann, "Range of novel black hole phase transitions via massive gravity: Triple points and N-fold reentrant phase transitions", Phys. Rev. D **101**, 8 084026 (2020). DOI: 10.1103/PhysRevD.101.084026

[16] C. V. Johnson, "Holographic Heat Engines", Class. Quant. Grav. **31**, 205002 (2014). DOI: 10.1088/0264-9381/31/20/205002

[17] B. P. Dolan, A. Kostouki, D. Kubiznak, and R. B. Mann, "Isolated critical point from Lovelock gravity", Class. Quant. Grav. 31, 24 242001 (2014). DOI: 10.1088/0264-9381/31/24/242001

[18] R. A. Hennigar, R. B. Mann, and E. Tjoa, "Superfluid Black Holes", Phys. Rev. Lett. **118**, 2 021301 (2017). DOI: 10.1103/PhysRevLett.118.021301

[19] Ökcü and E. Aydiner, "Joule–Thomson expansion of the charged AdS black holes", Eur. Phys. J. C **77**, 1 24 (2017). DOI: 10.1140/epjc/s10052-017-4598-y

[20] S.-W. Wei and Y.-X. Liu, "Insight into the Microscopic Structure of an AdS Black Hole from a Thermodynamical Phase Transition", Phys. Rev. Lett. **115**, 11 111302 (2015). [Erratum: Phys.Rev.Lett. 116, 169903 (2016)]. DOI: 10.1103/PhysRevLett.115.111302

[21] M. Tavakoli, J. Wu, and R. B. Mann, "Multi-critical points in black hole phase transitions", JHEP **12**, 117 (2022). DOI: 10.1007/JHEP12(2022)117

[22] J. Wu and R. B. Mann, "Multicritical Phase Transitions in Multiply Rotating Black Holes", Class. Quant. Grav. **40**, 6, 06LT01 (2023). DOI: 10.1088/1361-6382/acbc04

[23] J. Wu and R. B. Mann, "Thermodynamically stable phases of asymptotically flat Lovelock black holes", Class. Quant. Grav. **40**, 14 145009 (2023). DOI: 10.1088/1361-6382/acdd41

[24] M. Astorino, "Thermodynamics of Regular Accelerating Black Holes", Phys. Rev. D **95**, 6 064007 (2017). DOI: 10.1103/PhysRevD.95.064007

[25] A. Anabalón, M. Appels, R. Gregory, D. Kubizňák, R. B. Mann, and A. Ovgün, "Holographic Thermodynamics of Accelerating Black Holes", Phys. Rev. D **98**, 10 104038 (2018). DOI: 10.1103/PhysRevD.98.104038

[26] A. Anabalón, F. Gray, R. Gregory, D. Kubizňák, and R. B. Mann, "Thermodynamics of Charged, Rotating, and Accelerating Black Holes", JHEP **04**, 096 (2019). DOI: 10.1007/JHEP04(2019)096

[27] B. P. Dolan, D. Kastor, D. Kubiznak, R. B. Mann, and J. Traschen, "Thermodynamic Volumes and Isoperimetric Inequalities for de Sitter Black Holes", Phys. Rev. D **87**, 10 104017 (2013). DOI: 10.1103/PhysRevD.87.104017

[28] S. Mbarek and R. B. Mann, "Reverse Hawking-Page Phase Transition in de Sitter Black Holes", JHEP **02**, 103 (2019). DOI: 10.1007/JHEP02(2019)103

[29] F. Simovic and R. B. Mann, "Critical Phenomena of Charged de Sitter Black Holes in Cavities", Class. Quant. Grav. **36**, 1 014002 (2019). DOI: 10.1088/1361-6382/aaf445

[30] S. Mbarek and R. B. Mann, "Thermodynamic Volume of Cosmological Solitons", Phys. Lett. B **765**, 352–358 (2017). DOI: 10.1016/j.physletb.2016.12.042

[31] C. Quijada, A. Anabal´on, R. B. Mann, and J. Oliva, "Triple Points of Gravitational AdS Solitons and Black Holes", arXiv:2308.16341. DOI: 10.48550/arXiv.2308.16341

[32] G. W. Gibbons, M. J. Perry, and C. N. Pope, "The First law of thermodynamics for Kerr-anti-de Sitter black holes", Class. Quant. Grav. **22**, 1503–1526 (2005). DOI: 10.1088/0264-9381/22/9/002

[33] B. P. Dolan, "Bose condensation and branes", JHEP **10**, 179 (2014). DOI: 10.1007/JHEP10(2014)179

[34] D. Kastor, S. Ray, and J. Traschen, "Chemical Potential in the First Law for Holographic Entanglement Entropy", JHEP **11**, 120 (2014). DOI: 10.1007/JHEP11(2014)120

[35] J.-L. Zhang, R.-G. Cai, and H. Yu, "Phase transition and thermodynamical geometry for Schwarzschild AdS black hole in $AdS5 \times S$ spacetime", JHEP **02**, 143 (2015). DOI: 10.1007/JHEP02(2015)143

[36] J.-L. Zhang, R.-G. Cai, and H. Yu, "Phase transition and thermodynamical geometry of Reissner-Nordström-AdS black holes in extended phase space", Phys. Rev. D **91**, , no. 4 044028 (2015). DOI: 10.1103/PhysRevD.91.044028

[37] B. P. Dolan, "Pressure and compressibility of conformal field theories from the AdS/CFT correspondence", Entropy **18**, 169 (2016). DOI: 10.3390/e18050169

[38] F. McCarthy, D. Kubizňák, and R. B. Mann, "Breakdown of the equal area law for holographic entanglement entropy", JHEP **11**, 165 (2017). DOI: 10.1007/JHEP11(2017)165

[39] J. M. Maldacena, "The Large N limit of superconformal field theories and supergravity", Adv. Theor. Math. Phys. **2**, 231–252 (1998). DOI; 10.1023/A:1026654312961

[40] E. Witten, "Anti-de Sitter space and holography", Adv. Theor. Math. Phys. **2**, 253–291 (1998). DOI: 10.4310/ATMP.1998.v2.n2.a2

[41] E. Witten, "Anti-de Sitter space, thermal phase transition", and confinement in gauge theories, Adv. Theor. Math. Phys. **2**, 505–532 (1998). DOI: 10.4310/ATMP.1998.v2.n3.a3

[42] S. W. Hawking and D. N. Page, "Thermodynamics of Black Holes in anti-De Sitter Space", Commun. Math. Phys. **87**, 577 (1983). DOI: 10.1007/BF01208266

[43] E. Caceres, P. H. Nguyen, and J. F. Pedraza, "Holographic entanglement entropy and the extended phase structure of STU black holes", JHEP **09**, 184 (2015). DOI: 10.1007/JHEP09(2015)184

[44] A. Karch and B. Robinson, "Holographic Black Hole Chemistry", JHEP **12**, 073 (2015). DOI: 10.1007/JHEP12(2015)073

[45] M. Sinamuli and R. B. Mann, "Higher Order Corrections to Holographic Black Hole Chemistry", Phys. Rev. D **96**, no. 8 086008 (2017). DOI: 10.1103/PhysRevD.96.086008

[46] M. R. Visser, "Holographic thermodynamics requires a chemical potential for color", Phys. Rev. D **105**, no. 10 106014 (2022). DOI: 10.1103/PhysRevD.105.106014

[47] D. Kastor, S. Ray, and J. Traschen, "Smarr Formula and an Extended First Law for Lovelock Gravity", Class. Quant. Grav. **27**, 235014 (2010). DOI: 10.1088/0264-9381/27/23/235014

[48] W. Cong, D. Kubiznak, and R. B. Mann, "Thermodynamics of AdS Black Holes: Critical Behavior of the Central Charge", Phys. Rev. Lett. **127**, no. 9 091301 (2021). DOI: 10.1103/PhysRevLett.127.091301

[49] M. B. Ahmed, W. Cong, D. Kubizňák, R. B. Mann, and M. R. Visser, "Holographic Dual of Extended Black Hole Thermodynamics", Phys. Rev. Lett. **130**, no. 18 181401 (2023). DOI: 10.1103/PhysRevLett.130.181401

[50] S. S. Gubser, I. R. Klebanov, and A. M. Polyakov, "Gauge theory correlators from noncritical string theory", Phys. Lett. B **428**, 105–114 (1998). DOI: 10.1016/S0370-2693(98)00377-3

[51] G. Zeyuan and L. Zhao, "Restricted phase space thermodynamics for AdS black holes via holography", Class. Quant. Grav. **39**, 7, 075019 (2022). DOI: 10.1088/1361-6382/ac566c

[52] W. Cong, D. Kubiznak, R. B. Mann, and M. R. Visser, "Holographic CFT phase transitions and criticality for charged AdS black holes", JHEP **08**, 174 (2022). DOI: 10.1007/JHEP08(2022)174

[53] A. Chamblin, R. Emparan, C. V. Johnson, and R. C. Myers, "Charged AdS black holes and catastrophic holography", Phys. Rev. D **60**, 064018 (1999). DOI: 10.1103/PhysRevD.60.064018

[54] I. Savonije and E. P. Verlinde, "CFT and entropy on the brane", Phys. Lett. B **507**, 305–311 (2001). DOI: 10.1016/S0370-2693(01)00467-1

[55] M. B. Ahmed, W. Cong, D. Kubiznak, R. B. Mann, and M. R. Visser, "Holographic CFT phase transitions and criticality for rotating AdS black holes", JHEP **08**, 142 (2023). DOI: 10.1007/JHEP08(2023)142

[56] T.-F. Gong, J. Jiang, and M. Zhang, "Holographic thermodynamics of rotating black holes", JHEP **06**, 105 (2023). DOI: 10.1007/JHEP06(2023)105

[57] M. Zhang and J. Jiang, "Bulk-boundary thermodynamic equivalence: a topology viewpoint", JHEP **06**, 115 (2023). DOI: 10.1007/JHEP06(2023)115

[58] G. Arenas-Henriquez, A. Cisterna, F. Diaz, and R. Gregory, "Accelerating black holes in 2 + 1 dimensions: holography revisited", JHEP **09**, 122 (2023). DOI: 10.1007/JHEP09(2023)122

[59] A. Al Balushi, R. A. Hennigar, H. K. Kunduri, and R. B. Mann, "Holographic Complexity and Thermodynamic Volume", Phys. Rev. Lett. **126**, no. 10 101601 (2021). DOI: 10.1103/PhysRevLett.126.101601

[60] A. Al Balushi, R. A. Hennigar, H. K. Kunduri, and R. B. Mann, "Holographic complexity of rotating black holes", JHEP **05**, 226 (2021). DOI: 10.1007/JHEP05(2021)226

[61] A. Bernamonti, F. Bigazzi, D. Billo, L. Faggi, and F. Galli, "Holographic and QFT complexity with angular momentum", JHEP **11**, 037 (2021). DOI: 10.1007/JHEP11(2021)037

[62] M. Zhang, C. Fang, and J. Jiang, "Holographic complexity of rotating black holes with conical deficits", Phys. Lett. B **838**, 137691 (2023). DOI: 10.1016/j.physletb.2023.137691